

# Revealing anyonic features in a toric code quantum simulation

J. K. Pachos<sup>1</sup>, W. Wieczorek<sup>2,3</sup>, C. Schmid<sup>2,3</sup>, N. Kiesel<sup>2,3</sup>, R. Pohlner<sup>2,3</sup> and H. Weinfurter<sup>2,3</sup>

<sup>1</sup>School of Physics & Astronomy, University of Leeds, Leeds LS2 9JT, UK,

<sup>2</sup>Max-Planck-Institute of Quantum Optics, D-85748 Garching, Germany,

<sup>3</sup>Department for Physics, Ludwig-Maximilians-Universität München, D-80799 München, Germany.

## Abstract.

Anyons are quasiparticles in two-dimensional systems that show statistical properties very distinct from those of bosons or fermions. While their isolated observation has not yet been achieved, here we perform a quantum simulation of anyons on the toric code model. By encoding the model in the multi-partite entangled state of polarized photons, we are able to demonstrate various manipulations of anyonic states and, in particular, their characteristic fractional statistics.

PACS numbers: 05.30.Pr, 73.43.Lp, 03.65.Vf

## 1. Introduction

In three spatial dimensions, only two types of statistical behaviors have been observed dividing particles into two groups: bosons and fermions. If one is restricted to two-dimensional systems the situation changes. There, anyons [1] can appear, which exhibit fractional statistics that ranges continuously from bosonic to fermionic. Anyons are responsible for the fractional quantum Hall effect [2] and it has been demonstrated that they could be realized as quasiparticles in highly entangled many-body systems. Formally, the properties of anyons are described by two-dimensional topological quantum field theories [3] that dictate their trivial dynamical, but complex statistical behavior. In general, it is expected that such topological quantum field theories come into effect at low energies of highly correlated many-body systems, such as quantum liquids [4]. However, the observation of anyonic features requires high population in the system's ground state, high purity samples and, above all, the ability to separate the anyonic effects from the dynamical background of the strongly interacting system. In spite of significant experimental progress [5] the fractional statistics of anyons has not yet been conclusively confirmed due to the complexity of these systems [6].

To demonstrate characteristic anyonic features we employ here a different strategy. We simulate the toric code model [7] in a quantum system without the continuous presence of interactions [8]. The toric code is a two-dimensional topological lattice model, where anyons are spatially well localized. Recently, several proposals showed how the toric code could possibly be implemented on extended lattices of qubits enabling one to employ anyonic states for, e.g., protected quantum computation [9]. While such a quantum computational scheme requires large systems, here we show that a number of anyonic properties can be demonstrated by considering four-partite entangled Greenberger-Horne-Zeilinger (GHZ) states [10]. These states are dynamically encoded in the polarization of photons, rather than produced via cooling [8]. This provides the additional advantage of being subject to negligible decoherence due to the weak coupling of photons to the environment. Polarized photons as qubits are a well understood and controllable quantum optical system that already allowed to observe the four-qubit GHZ state [11]. Here we employ this system to simulate anyonic behavior.

## 2. Toric code model

### 2.1. Hamiltonian and ground state

The anyonic model under consideration is based on the toric code proposed by Kitaev [7] and is described in detail in tutorial introductions [12]. This system can be defined on a two-dimensional square lattice with interacting qubits placed at its vertices. To facilitate the description of the interactions let us split the lattice into two alternating types of plaquettes labelled by  $p$  and  $s$ , as in figure 1. The defining Hamiltonian is

$$\mathcal{H} = - \sum_p \sigma_{p,1}^z \sigma_{p,2}^z \sigma_{p,3}^z \sigma_{p,4}^z - \sum_s \sigma_{s,1}^x \sigma_{s,2}^x \sigma_{s,3}^x \sigma_{s,4}^x , \quad (1)$$

where the summations run over the corresponding plaquettes and the indices 1, ..., 4 of the Pauli operators,  $\sigma^z$  and  $\sigma^x$ , enumerate the vertices of each plaquette in a counter-clockwise fashion. Each of the  $s$ - or  $p$ -plaquette interaction terms commute with the Hamiltonian as well as with each other. Thus, the model is exactly solvable and its ground state is explicitly given by [13]

$$|\xi\rangle = \prod_s \frac{1}{\sqrt{2}} (\mathbb{1} + \sigma_{s,1}^x \sigma_{s,2}^x \sigma_{s,3}^x \sigma_{s,4}^x) |00\dots 0\rangle, \quad (2)$$

with  $\sigma^z|0\rangle = |0\rangle$ . The state  $|\xi\rangle$  represents the anyonic vacuum state and it is unique for systems with open boundary conditions.

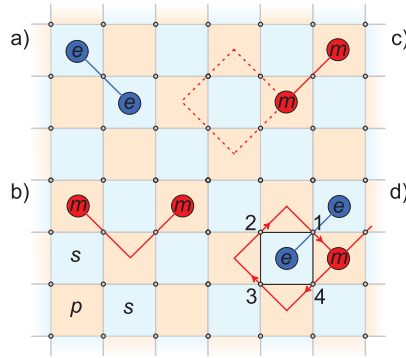


**Figure 1.** The toric code lattice with qubits at the vertices of a square lattice with two types of plaquettes. Light blue and red plaquettes correspond to the  $s$ - and  $p$ -plaquettes, respectively. Qubit rotations enable manipulations of anyons on neighboring plaquettes. (a) Application of  $\sigma^z$  on a single qubit yields two  $e$ -type anyons placed at the neighboring  $s$  plaquettes, where the string passes through the rotated qubits. Similarly,  $m$  anyons are created on  $p$  plaquettes by  $\sigma^x$  rotations. (b) Two  $\sigma^x$  rotations create two pairs of  $m$ -type anyons. If one anyon from each pair is positioned on the same plaquette then they annihilate, thereby connecting their strings. (c) When a part of a string forms a loop around unpopulated plaquettes, the loop cancels (dashed). (d) Here we restrict to one  $s$  plaquette and four neighboring  $p$  plaquettes. Anyon  $e$  is produced by a  $\sigma^z$  on qubit 1 (blue),  $|e\rangle = \sigma_1^z |\xi\rangle$ . This system can support the circulation of an  $m$  around an  $e$  anyon.

## 2.2. Anyonic quasiparticles

Starting from this ground state one can excite pairs of anyons connected by a string on the lattice using single qubit operations. More specifically, by applying  $\sigma^z$  on some qubit of the lattice a pair of so called  $e$ -type anyons is created on the two neighboring  $s$  plaquettes [figure 1(a)] and the system is described by the state  $|e\rangle = \sigma^z |\xi\rangle$ . An  $m$  pair of anyons lives on the  $p$  plaquettes and is obtained by a  $\sigma^x$  operation. The combination of both creates the composite quasiparticle  $\epsilon$  with  $|\epsilon\rangle = \sigma^z \sigma^x |\xi\rangle = i \sigma^y |\xi\rangle$ . Two equal Pauli rotations applied on qubits of the same plaquette create two anyons on this plaquette. The fusion rules ( $1 \times 1 = e \times e = m \times m = \epsilon \times \epsilon = 1$ ,  $e \times m = \epsilon$ ,  $1 \times e = e$ , etc., where 1 is the vacuum state [12]) describe the outcome from combining

two anyons. In the above example, if two anyons are created on the same plaquette then they annihilate. This operation also glues two single strings of the same type together to form a new string, again with a pair of anyons at its ends [Figure 1(b)]. If the string forms a loop, the anyons at its end annihilate each other, thus removing the anyonic excitation. In case that only a part of the string forms a loop, the string gets truncated [Figure 1(c)]. For non-compact finite systems, such as the one we consider here, a string may end up at the boundary describing a single anyon at its free endpoint.

### 2.3. Anyonic statistics

Anyonic statistics is revealed as a non-trivial phase factor acquired by the wave function of the lattice system after braiding anyons, i.e., after moving an  $m$  anyon around an  $e$  anyon [Figure 1(d)] or vice versa. Consider the initial state  $|\Psi_{\text{ini}}\rangle = \sigma_1^z |\xi\rangle = |e\rangle$ . If an anyon of type  $m$  is assumed to be at a neighboring  $p$  plaquette it can be moved around  $e$  along the path generated by successive applications of  $\sigma^x$  rotations on the four qubits of the  $s$  plaquette. The final state is

$$|\Psi_{\text{fin}}\rangle = \sigma_1^x \sigma_2^x \sigma_3^x \sigma_4^x |\Psi_{\text{ini}}\rangle = -\sigma_1^z (\sigma_1^x \sigma_2^x \sigma_3^x \sigma_4^x |\xi\rangle) = -|\Psi_{\text{ini}}\rangle. \quad (3)$$

Such a minimal loop, which vanishes the moment it is closed, is analogous to the application of the respective interaction term  $C_s = \sigma_{s,1}^x \sigma_{s,2}^x \sigma_{s,3}^x \sigma_{s,4}^x$  (or  $C_p = \sigma_{p,1}^z \sigma_{p,2}^z \sigma_{p,3}^z \sigma_{p,4}^z$ ) of the Hamiltonian. This operator has eigenvalue  $+1$  for all plaquettes of the ground state  $|\xi\rangle$ , whereas it signals an excitation, e.g.,  $|\Psi_{\text{ini}}\rangle$ , with eigenvalue  $-1$ , when applied to the plaquette where an anyon resides. However, (3) is much more general, as the actual path of the loop is irrelevant. It is the topological phase factor of  $-1$ , which reveals the presence of the enclosed anyon. Alternatively, we can interpret (3) as a description of twisting  $\epsilon$ , the combination of an  $e$  and an  $m$ -type anyon, by  $2\pi$ . The phase factor of  $-1$  thereby reveals its  $4\pi$ -symmetry, characteristic for half spin, fermionic particles [14]. Note that the  $e$  ( $m$ ) anyons exhibit bosonic statistics with respect to themselves [7].

## 3. Experimental implementation

### 3.1. Minimal instance of the toric code model

As this two-dimensional system is well suited for demonstrating characteristic anyonic features, the question arises how big the lattice has to be. It turns out that four qubits of a single  $s$  plaquette represent the minimal unit of the toric code model [15]. In this case, the four neighboring  $p$  plaquettes are represented only by their corresponding links. Hence, while the presence of an  $e$  anyon is detected by the plaquette operator  $C_s$ , the presence of  $m$  anyons is detected by the eigenvalue of the four  $C'_p = \sigma_{p,i}^z \sigma_{p,j}^z$  operators that correspond to the adjacent links of the  $p$  plaquettes. Consequently, the product determining the ground state [Eqn. (2)] reduces to only one factor for the single  $s$ -plaquette resulting in a four qubit GHZ state,  $|\xi\rangle = (|0000\rangle + |1111\rangle)/\sqrt{2}$ . This is an

eigenstate of the relevant  $C_s$  and  $C'_p$  operators with eigenvalue  $+1$ . An eigenvalue  $-1$  for any of these operators denotes the presence of the corresponding anyon.

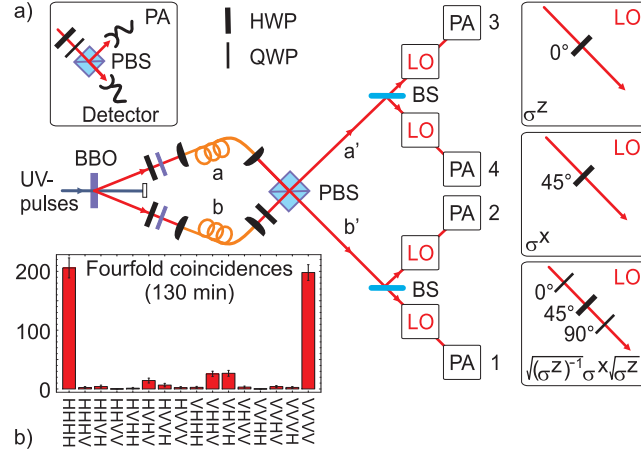


**Figure 2.** (a) The experimental set-up for the observation of the anyonic vacuum state of the toric code model, the demonstration of anyonic features and the verification of anyonic statistics. The photons are created in a 2 mm thick  $\beta$  Barium Borate (BBO) crystal, which is pumped by femtosecond ultraviolet (UV) pulses. Walk-off effects are compensated for by a HWP and a 1 mm thick BBO crystal. For the observation of the anyonic states, we are interested in the second order emission of the SPDC [16], initially emitted in the two spatial modes  $a$  and  $b$ :  $\propto |2H\rangle_a |2V\rangle_b + |2V\rangle_a |2H\rangle_b + |HV\rangle_a |HV\rangle_b$ . The photons are further processed by a HWP in mode  $b$ , which transforms  $|H\rangle$  into  $|+\rangle$  and  $|V\rangle$  into  $|-\rangle$  [with  $|\pm\rangle = (|H\rangle \pm |V\rangle)/\sqrt{2}$ ]. The state  $|\xi\rangle$  is observed behind the PBS and the BSs under the condition of detecting a photon in each of the four modes 1, 2, 3, 4 (average count rate:  $2.8 \text{ min}^{-1}$ ). The local operations (LO) for the demonstration of anyonic features are implemented by operation specific HWPs and quarter-wave plates (QWPs). The polarization state of each photon is analyzed (PA) with a HWP and a QWP in front of a PBS. (b) Measurement outcomes of  $|\xi\rangle$  in the basis  $\sigma_i^z$  for each qubit.

### 3.2. State implementation

In our simulation the qubits supporting the anyonic states are encoded in the polarization of single photons propagating in well-defined spatial modes. This means that for the anyonic vacuum and for all obtained final states our system is of the form  $|\text{GHZ}^\phi\rangle = (|H_1 H_2 H_3 H_4\rangle + e^{i\phi} |V_1 V_2 V_3 V_4\rangle)/\sqrt{2}$ . The indices (omitted in the following) label the spatial mode of each photon, i.e., they represent the position of the qubit as in Figure 1(d), and H (V) denote linear horizontal (vertical) polarization, representing a logical 0 (1). To obtain such four-photon entangled states, the second order emission of a non-collinear type-II spontaneous parametric down conversion process (SPDC) [17], yielding four photons in two spatial modes, is overlapped on a polarizing beam splitter (PBS) and afterwards symmetrically split up into four spatial modes by two polarization independent beam splitters (BS), see Figure 2(a) [18]. Prior to the second order interference at the PBS the polarization of two of the photons is rotated by a

half-wave plate (HWP). Under the condition of detecting one photon in each spatial mode we observe the desired states.

As we are interested in the vacuum  $|\xi\rangle = |\text{GHZ}^0\rangle$  and the anyonic state  $|e\rangle = \sigma_i^z|\xi\rangle = |\text{GHZ}^\pi\rangle$ , the successful simulation and demonstration of anyonic features relies on a careful distinction and characterization of these two orthogonal GHZ states. This comprises the confirmation of genuine four-partite entanglement and a method to reveal the phase  $\phi$ . For this purpose, state analysis is performed by measuring the correlation,  $c_z$ , in the  $\sigma_i^z$  basis for each qubit and the correlation function  $c_{xy}(\gamma) = \sigma_1(\gamma) \otimes \sigma_2(\gamma) \otimes \sigma_3(\gamma) \otimes \sigma_4(\gamma)$  with  $\sigma_i(\gamma) = [(\cos \gamma)\sigma_i^y + (\sin \gamma)\sigma_i^x]$  [19]. This measurement is ideally suited to prove the coherent superposition of the terms  $|\text{HHHH}\rangle$  and  $|\text{VVVV}\rangle$  and to determine their relative phase  $\phi$ . It is obtained from a measurement of all qubits along the same direction in the  $x$ - $y$  plane of the Bloch sphere. For a  $\text{GHZ}^\phi$  state its expectation value shows an oscillation,  $\langle c_{xy}(\gamma) \rangle = \mathcal{V} \cos(4\gamma + \phi)$ , with a period of one quarter of  $2\pi$ . This is a unique signature of four qubit GHZ entanglement. The visibility of this oscillation  $\mathcal{V}$  is 1 for pure GHZ states. For a general state it equals twice the element  $\rho_{\text{HHHH}, \text{VVVV}} = \text{Tr}(|\text{HHHH}\rangle\langle \text{VVVV}| \rho)$  of the corresponding density matrix  $\rho$ .

To analyze the performance of the set-up, first, the observation of the state  $|\xi\rangle = |\text{GHZ}^0\rangle$  is confirmed. Figure 2(b) shows all possible measurement outcomes in the  $\sigma_1^z \sigma_2^z \sigma_3^z \sigma_4^z$  basis, where the expected populations of  $|\text{HHHH}\rangle$  and  $|\text{VVVV}\rangle$  are clearly predominant with probabilities of  $P_{\text{HHHH}} = (41.2 \pm 3.4)\%$  and  $P_{\text{VVVV}} = (39.6 \pm 2.7)\%$ , respectively, close to the expected  $P_{\text{HHHH}} = P_{\text{VVVV}} = 50\%$ . We find a correlation of  $\langle c_z \rangle = 0.908 \pm 0.047$ . The population of other terms is caused by noise arising from higher-order emissions of the down conversion and a remaining degree of distinguishability of photons at the PBS. The dependence of  $\langle c_{xy}(\gamma) \rangle$  for the state  $|\xi\rangle$  is displayed in Figure 3(a) from which we infer a visibility  $\mathcal{V}$  of  $(68.3 \pm 1.1)\%$ . This value is obtained from a weighted least squares fit to a Fourier decomposition of  $\langle c_{xy}(\gamma) \rangle$  considering only even components up to order 4:  $\langle c_{xy}(\gamma) \rangle = \sum_{k=0}^2 a_k \cos(2k \cdot \gamma) + b_k \sin(2k \cdot \gamma)$ . Only these components can originate from physical states. From the phase of the correlation function we deduce the phase of the  $\text{GHZ}^0$  state to be  $\phi = (0.02 \pm 0.01)\pi$ , close to the expected value of 0.

The visibility  $\mathcal{V}$  together with the populations  $P_{\text{HHHH}}$  and  $P_{\text{VVVV}}$  allow further to determine the fidelity  $F = \langle \text{GHZ} | \rho | \text{GHZ} \rangle = (\mathcal{V} + P_{\text{HHHH}} + P_{\text{VVVV}})/2$ . We obtain a value of  $(74.5 \pm 2.2)\%$  (for measurement data see also Table 1). The fidelity is not only important for an estimation of state quality but can also be applied to verify genuine four-partite entanglement, an essential element in the presented toric code model. With a proper entanglement witness a fidelity greater than 50% is sufficient [20]. The experimentally observed fidelity is clearly above this bound, i.e., it is of high enough quality to allow for the demonstration of the anyonic properties.

### 3.3. Anyonic manipulations and detection of anyonic statistics

We start by analyzing the state change under the creation (and annihilation) of anyons, thereby demonstrating the characteristic fusion rules. Applying  $\sigma_1^z$  in mode 1 creates an  $e$ -type anyon on the  $s$  plaquette resulting in a  $\text{GHZ}^\pi$  state, Figure 3(b). This is clearly proven by the phase  $\phi = 1.02\pi$  of the correlation function. A further application of  $\sigma_j^z$  on any other mode, say  $j = 3$ , changes the state of the plaquette according to  $e \times e = 1$ , and the anyon is moved away from the  $s$  plaquette under investigation. These two  $\sigma^z$  rotations represent a string connecting two anyons, which traverses the particular plaquette without influencing its state, as confirmed by the observation of the initial  $\text{GHZ}^0$  state [ $\phi = 0.01\pi$ , Figure 3(c)]. A further  $\sigma_j^z$  rotation on one of the remaining vertices, e.g.,  $j = 4$ , creates an  $e$  occupation on the plaquette. Thus, the observation of  $\text{GHZ}^\pi$  [ $\phi = 1.03\pi$ , Figure 3(d)] demonstrates the non-trivial version of the  $1 \times e = e$  fusion rule. Alternatively, this can be seen as demonstrating the invariance of an anyonic state, when a string traverses the plaquette.

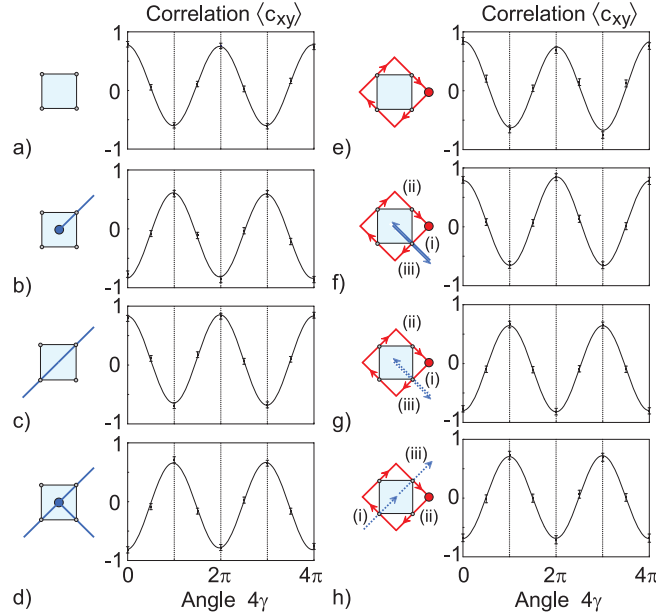


**Figure 3.** Pictorial representations of various evolutions of anyons, together with the correlation function  $\langle c_{xy} \rangle$ . The phase of  $\langle c_{xy} \rangle$  directly gives the phase  $\phi$  of  $|\text{GHZ}^\phi\rangle$ . (a) The vacuum state,  $|\xi\rangle$ . (b) Generating an  $e$ -type anyonic state  $|e\rangle = |\text{GHZ}^\pi\rangle$  by a  $\sigma^z$  operator. (c) A second  $\sigma^z$  removes the anyon from the plaquette and elongates the string resulting in the  $\text{GHZ}^0$  state. (d) A third  $\sigma^z$  creates another pair of anyons, connected with the string already traversing the plaquette. (e) Moving an  $m$  anyon around an empty  $s$  plaquette or (f) first creating an  $e$  anyon on the plaquette (i), performing the loop (ii), and removing the  $e$  anyon from the plaquette again (iii) give identical final states up to a global phase factor. (g) The global phase,  $\pi$ , is revealed by superimposing the two above evolutions, thereby clearly proving anyonic statistics. (h) An alternative path for the anyon  $e$  that gives the same fractional statistical phase,  $\pi$ .

To detect the major feature of anyons, their non-trivial statistical phase acquired when moving one anyon around the other, we employed an interference measurement, which makes their *overall* phase factor visible [see (3) and Figure 1(d)]. Let us study the two evolutions separately. The first is to create a pair of two  $m$  anyons, move one of them around the empty  $s$  plaquette and then annihilate them. This evolution is equivalent to having a string ending up at a  $p$  plaquette with an  $m$  anyon at its endpoint and circulating that anyon around the  $s$  plaquette. The obtained loop operator  $C_s$ , obviously, does not change the vacuum state and, thus, results in  $\text{GHZ}^0$  [ $\phi = -0.02\pi$ , Figure 3(e)]. Alternatively, we (i) create an  $e$  anyon on the plaquette, (ii) encompass it with the loop of an  $m$  anyon, and (iii) remove it again [Figure 3(f)]. The whole evolution is, in analogy to (3), described by  $\sigma_4^z(\sigma_1^x\sigma_2^x\sigma_3^x\sigma_4^x)\sigma_4^z|\xi\rangle = -|\xi\rangle = -|\text{GHZ}^0\rangle$ . The correlation function determines faithfully the angle  $\phi = -0.01\pi$  [Figure 3(f)], but is blind to the characteristic overall phase factor. This, finally, can be observed by (i) first generating the *superposition*  $e^{-i\pi/4}(|\xi\rangle + i|e\rangle)/\sqrt{2}$  of having an anyon  $e$  on the plaquette or not by the unitary operation  $(\sigma_i^z)^{-1/2}$ ; (ii) moving the  $m$  anyon around this superposition gives  $e^{-i\pi/4}(|\xi\rangle - i|e\rangle)/\sqrt{2}$ , the superposition of the above evolutions; and (iii) the application of the inverse rotation  $(\sigma_i^z)^{1/2}$  makes the phase difference visible resulting in  $-i|e\rangle = -i|\text{GHZ}^\pi\rangle$ . The observed value of  $\phi = 1.00\pi$  [Figure 3(g)] clearly proves the phase acquired by the braiding and therefore the anyonic statistics [21]. To reinforce the observation of the obtained fractional phase, we perform an additional interference experiment with an alternative path. Now, the superposition of an  $e$  anyonic state and the ground state is generated in the  $s$ -plaquette by rotating one qubit and it is removed by rotating another qubit, as seen in Figure 3(h). If we move an  $m$  anyon around the plaquette in between the two steps, we observe *again* the characteristic phase shift of  $-1$ .

#### 4. Conclusions

Our results show that we can create, manipulate and detect the toric code states by encoding them in a simple physical system. In our quantum simulation we demonstrated several of the fusion rules and we provided supporting evidence for the fractional statistics of the toric code anyons. Multiqubit toric code states are known to be useful for novel types of quantum error correction [22]. Extending our experimental results presented here to larger, scalable quantum systems [23, 24] will enable the application of the toric code for quantum information processing in the future [25].

Note added: With the completion of this work we became aware of a similar experimental implementation, closely resembling [8], that was simultaneously performed [26].



	Phase $\phi$	Fidelity $F$
Vacuum state		
$ \xi\rangle$	$(0.02 \pm 0.01) \cdot \pi$	$(74.5 \pm 2.2)\%$
Creation of a single $e$ -type anyon		
$\sigma_1^z  \xi\rangle$	$(1.02 \pm 0.01) \cdot \pi$	$(74.9 \pm 2.8)\%$
$\sigma_2^z  \xi\rangle$	$(1.00 \pm 0.01) \cdot \pi$	$(74.2 \pm 2.7)\%$
$\sigma_3^z  \xi\rangle$	$(1.01 \pm 0.01) \cdot \pi$	$(76.5 \pm 3.2)\%$
$\sigma_4^z  \xi\rangle$	$(0.97 \pm 0.02) \cdot \pi$	$(76.2 \pm 3.7)\%$
String passing through the $s$ plaquette		
$\sigma_1^z \sigma_2^z  \xi\rangle$	$(0.02 \pm 0.01) \cdot \pi$	$(77.4 \pm 2.8)\%$
$\sigma_1^z \sigma_3^z  \xi\rangle$	$(0.01 \pm 0.01) \cdot \pi$	$(77.3 \pm 2.5)\%$
$\sigma_1^z \sigma_4^z  \xi\rangle$	$(-0.01 \pm 0.01) \cdot \pi$	$(76.3 \pm 2.6)\%$
String passing through the $s$ plaquette populated with an anyon		
$\sigma_2^z \sigma_4^z  e\rangle$	$(1.02 \pm 0.01) \cdot \pi$	$(75.2 \pm 2.4)\%$
$\sigma_3^z \sigma_4^z  e\rangle$	$(1.03 \pm 0.01) \cdot \pi$	$(76.7 \pm 2.7)\%$
$\sigma_1^z \sigma_4^z  e\rangle$	$(1.02 \pm 0.02) \cdot \pi$	$(74.5 \pm 3.1)\%$
Loop around an unpopulated $s$ plaquette		
$C_s  \xi\rangle$	$(-0.02 \pm 0.02) \cdot \pi$	$(76.6 \pm 3.4)\%$
Loop around a populated $s$ plaquette followed by annihilation of the anyon		
$(\sigma_4^z) C_s (\sigma_4^z)  \xi\rangle$	$(-0.01 \pm 0.01) \cdot \pi$	$(76.8 \pm 2.8)\%$
Interference procedure to reveal anyonic statistics		
$(\sigma_1^z)^{1/2} C_s (\sigma_1^z)^{-1/2}  \xi\rangle$	$(1.03 \pm 0.01) \cdot \pi$	$(76.1 \pm 3.0)\%$
$(\sigma_2^z)^{1/2} C_s (\sigma_2^z)^{-1/2}  \xi\rangle$	$(0.99 \pm 0.01) \cdot \pi$	$(73.5 \pm 3.6)\%$
$(\sigma_3^z)^{1/2} C_s (\sigma_3^z)^{-1/2}  \xi\rangle$	$(1.01 \pm 0.01) \cdot \pi$	$(75.2 \pm 3.0)\%$
$(\sigma_4^z)^{1/2} C_s (\sigma_4^z)^{-1/2}  \xi\rangle$	$(1.00 \pm 0.01) \cdot \pi$	$(75.8 \pm 2.5)\%$
$(\sigma_1^z)^{1/2} C_s (\sigma_3^z)^{-1/2}  \xi\rangle$	$(1.00 \pm 0.01) \cdot \pi$	$(78.7 \pm 3.2)\%$

**Table 1.** Experimental measurement data of the anyonic states.

## Acknowledgments

We would like to thank Phillipe Grangier, Peter Zoller and Robert Raussendorf for inspiring conversations. We acknowledge the support of this work by EPSRC, the Royal Society, the DFG-Cluster of Excellence MAP and the EU Projects QAP, EMALI and SCALA. W.W. acknowledges support by QCCC of the Elite Network of Bavaria and the Studienstiftung des dt. Volkes.

## References

- [1] Wilczek F 1982 Phys. Rev. Lett. **48**, 1144.
- [2] Tsui D C, Stormer H L, and Gossard A C 1982 Phys. Rev. Lett. **48**, 1559.
- [3] Witten E 1989 Commun. Math. Phys. **121**, 351.

- [4] Anderson P W 1987 Science **235**, 1196.
- [5] Camino F E, Zhou W, and Goldman V J 2007 Phys. Rev. Lett. **98**, 076805.
- [6] Kim E-A 2006 Phys. Rev. Lett. **97**, 216404.
- [7] Kitaev A 2003 Ann. Phys. (N.Y.) **303**, 2.
- [8] Han Y-J, Raussendorf R, and Duan L-M 2007 Phys. Rev. Lett. **98**, 150404.
- [9] Jiang L et al. 2008 Nat. Phys. **4**, 482.
- [10] Greenberger D M, Horne M A, and Zeilinger A 1989 in *Bell's Theorem, Quantum Theory, and Conceptions of the Universe* (ed. Kafatos, M.) 73-76 (Kluwer Academic, Dordrecht).
- [11] Pan J W, et al. 2001 Phys. Rev. Lett. **86**, 4435.
- [12] Preskill J Lecture Notes for Physics 219: Quantum Computation, <http://www.theory.caltech.edu/~preskill/>.
- [13] Verstraete F, et al. 2006 Phys. Rev. Lett. **96**, 220601.
- [14] Rauch H, et al. 1975 Phys. Lett. A **54**, 425.
- [15] Pachos J K 2007 Ann. Phys. **322**, 1254.
- [16] Eibl M, et al. 2003 Phys. Rev. Lett. **90**, 200403.
- [17] Kwiat P G, et al. 1995 Phys. Rev. Lett. **75**, 4337.
- [18] Wieczorek W et al. 2008 Phys. Rev. Lett. **101**, 010503.
- [19] Sackett C A, et al. 2000 Nature **404**, 256.
- [20] Toth G, and Gühne O 2005 Phys. Rev. Lett. **94**, 060501.
- [21] Note that during the braiding evolution no dynamical phases are generated as there is no Hamiltonian present and the Pauli rotations are performed with zero order wave plates, thus, adding insignificant erroneous phases.
- [22] Kitaev A 1997 Russian Math. Surveys, **52** 1191.
- [23] Raussendorf R, Bravyi S, and Harrington J 2005 Phys. Rev. A **71**, 062313.
- [24] Micheli A, Brennen G K, and Zoller P 2006 Nature Physics **2**, 341.
- [25] Freedman M H, Kitaev A, Larsen M J, and Wang Z 2003 Bull. Amer. Math. Soc. **40**, 31.
- [26] Lu C-Y, et al. 2009, Phys. Rev. Lett. **102** 030502.